ASIA-PACIFIC SOLAR RESEARCH CONFERENCE

PEER REVIEWED
ASIA-PACIFIC
SOLAR RESEARCH CONFERENCE

Design of a heliostat field and liquid sodium cylindrical receiver for the Gen3 Liquids Pathway

Charles-Alexis Asselineau, William Logie, John Pye, Felix Venn, Shuang Wang and Joe Coventry

Solar Thermal Group (STG)
Research School of Electrical, Energy and Materials Engineering (RSEEME)
Craig building 35A, Science Road, The Australian National University, Canberra ACT 2600

The design methodology for a large-scale surround-type heliostat field and cylindrical receiver is presented in this study. Using this methodology, a 540 MW_{th} liquid sodium receiver concept and complementary heliostat field are established and their annual performances characterised in detail. The designs introduced in this study were taken to the US DOE and selected against a competing chloride-salts-based design form the US National Renewable Energy Laboratory NREL.

1. Introduction

The Australian Solar Thermal Research Institute (ASTRI), as a partner in the DOE Gen3 Liquids Pathway program, is evaluating an alternative receiver configuration using liquid sodium instead of chloride salts as the heat transfer fluid. In the Gen3 Liquids Pathway, thermal energy is stored as sensible heat in chloride salts; consequently, the receiver operates between 520°C and 740°C; slightly higher than its chloride salt counterpart to allow for unavoidable temperature drops in a sodium-salt heat exchanger. In this study, we present the 540 MWth cylindrical receiver and field design that was taken to the receiver down-selection meeting in February 2020 [1].

2. Sodium receiver system design methodology

2.1. Heliostat field design

The heliostat field layout (Figure 1), located in Daggett (CA, USA), was established using an in-house system-design code with the objective of maximizing the annual optical efficiency. This code uses Python to interface between ray-tracing (Solstice software from CNRS PROMES [1, 2]), the Single Objective Genetic Algorithm (SOGA) from the DAKOTA library from Sandia National Laboratories [4] and annual simulation integration routines based on Bi-cubic spline interpolation [5]. At this stage of the design, the aiming strategy is simplified and considers a single peak flux constraint. For ease of comparison with other teams in the project, a relatively simple limb-darkened sunshape, less prone to model-based discrepancies, was used. Using a fixed tower height, the receiver diameter was set at this point, while its height was later modified.

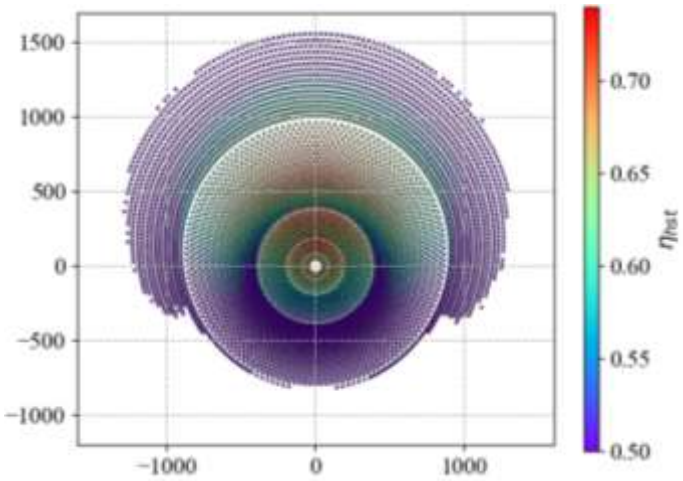

Figure 1: Heliostat field design obtained from the Single Objective Genetic Algorithm approach.

2.2. Receiver pipe selection and thermomechanical limits.

The combination of high-temperatures and the use of liquid sodium impose strict restrictions on the alloys that can be used for the receiver. Both Alloy 230 and Alloy 740H were considered, with the latter chosen for its superior strength. The ASME Section VIII elastic ratcheting analysis method was used to generate mass-flow and temperature dependent maximum allowable flux tables for a given tube geometry [6], which were then used to refine the geometry and establish the aiming strategy.

2.3. Receiver flow-path design

There is little information about sodium flow in pipes at temperatures compatible with the Gen3 Liquids Pathway; however, it is known that several corrosion mechanisms observed depend on flow velocities. In the sodium and NaK handbook [7], maximum velocities of 2.44 m/s are recommended, albeit for very different operating conditions. In the absence of better data, this value was assumed as a design constraint. The optimal flow-path for the receiver is obtained by running a series of parametric studies to determine the minimum number of banks and flow-paths able to meet this constraint. Using a set of simplified assumptions regarding the geometry, efficiency and flux distributions, it is possible to obtain an upper bound for the expected maximal flow velocity and select the least complex configuration that respects the design limit.

2.4. Final receiver geometry

The final geometry of the receiver was obtained by running detailed studies on selected receiver height, this time using the annual system efficiency as an objective function. A fast receiver energy balance model in Python and a new aiming strategy method based on an efficient parameterisation of the aiming problem [8] were here coupled with ray-tracing, considering thermomechanical limits, to evaluate the annual performance and establish the final design. The resulting receiver flux map at design point, is presented in Figure 2.

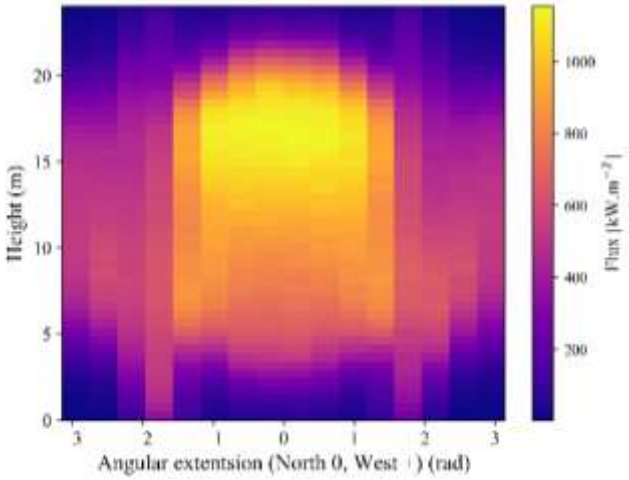

Figure 2: Receiver flux map at design point (Equinox solar noon) showing the prescribed non-uniform aiming on the receiver surface.

3. Results

The resulting receiver is 16 m in diameter and 24 m high (active tubing section) for a fixed tower height of 175 m (bottom of the receiver) and a field of 6764 heliostats. The heliostats are 12.2 m by 12.2 m, with overall optical error of 1.5 mrad and reflectance of 90%. The receiver itself is composed of 16 banks, each with 51 pipes of OD 60.3 mm and wall thickness 1.2 mm. The receiver is divided into 8 flow paths, with top north side injection and exit at the opposing top south location. Several studies were made with different convective heat loss correlations and coating absorptance values. In each case, the sodium receiver demonstrated higher performance than the salt counterpart with lower capital cost. Figure 3 shows some key results of the full energy, mass and momentum balance for the first flow-path at design point and Figure 4 shows a summary of the receiver performance for 3 key sun positions and the annually averaged values.

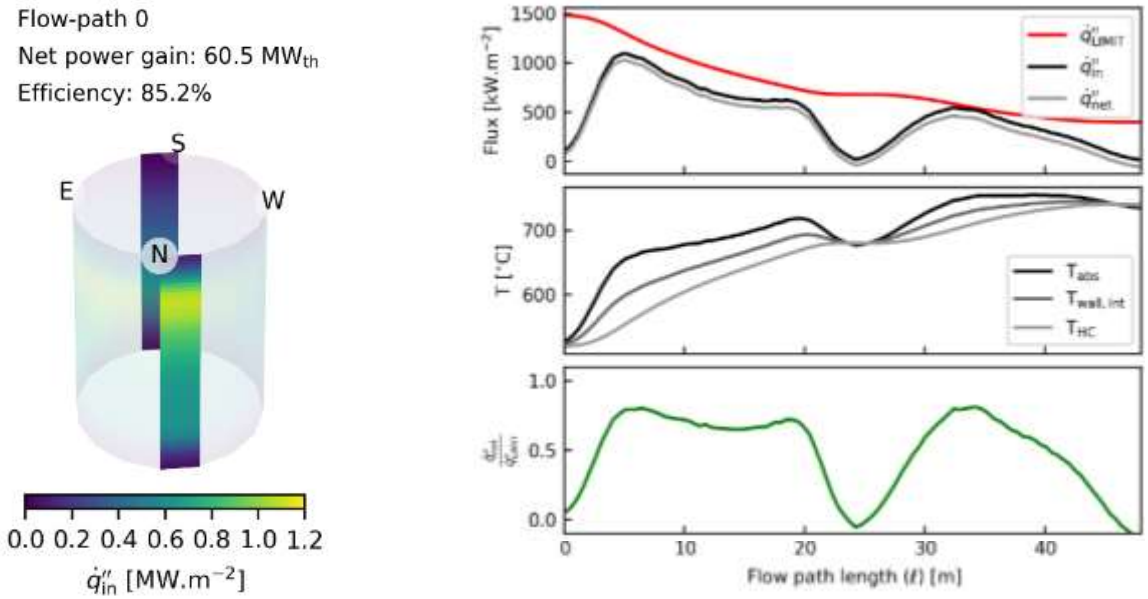

(a) **(b)**

Figure 3: Extract of receiver modelling results: (a) incident flux on a flow-path 0 and (b), from top to bottom, flux, temperature and fraction of allowable flux along flow-path 0 at design point.

Efficiency	Equinox noon	Summer noon	Winter noon	Annual
η_{field}	65.2%	66.4%	61.3%	54.8%
$\eta_{intercept}$	96.3%	96.8%	95.7%	
$\eta_{absorption}$	98.7%	98.7%	98.7%	
$\eta_{thermal}$	89.1%	89.2%	87.7%	
$\eta_{receiver}$	87.9%	88.0%	86.5%	
$\eta_{intercept}\eta_{receiver}$	84.7%	85.2%	82.8%	79.9%
$\eta_{overall}$	55.2%	56.6%	50.7%	43.8%

Figure 4: Extract of the annual efficiency evaluation with Equinox (design point), Summer solstice and Winter solstice performance at solar noon, and annual performances.

4. Next steps

Work is now ongoing to refine the receiver, field and tower arrangement concept. Among other aspects, the evaluation of systems with 2 to 4 towers is being conducted. The costing information for some of the most expensive items (tower, heat exchanger, etc.) is also being investigated to improve the accuracy of LCOE calculations.

References

[1] C. Turchi, C. Libby, J. Pye, and J. Coventry, “Liquid-Phase Pathway to SunShot: Receiver Selection using the Analytic Hierarchy Process,” in *Abstract, SolarPACES 2020*.

[2] J. Delatorre *et al.*, “Monte Carlo advances and concentrated solar applications,” *Sol. Energy*, vol. 103, no. 0, pp. 653–681, 2014.

[3] CNRS-PROMES and Meso-Star, “Solstice Software.” .

[4] B. M. Adams, “DAKOTA, a multilevel parallel object-oriented framework for design optimization, parameter estimation, uncertainty quantification, and sensitivity analysis,” 2009.

[5] V. Grigoriev, C. Corsi, and M. Blanco, “Fourier sampling of sun path for applications in solar energy,” in *AIP Conference Proceedings*, 2016, vol. 1734, no. 1, p. 20008.

[6] W. Logie, S. Jape, J. Martinek, J. Pye, J. Coventry, and C. Turchi, “Structural Integrity Assessment of Advanced Solar Central Receiver Alloy 740H Tubes,” in *Abstract, SolarPACES 2020*.

[7] O. J. Foust, *Sodium-NaK engineering handbook*. New York: Gordon and Breach, 1972.

[8] S. Wang, C.-A. Asselineau, J. Pye, and J. Coventry, “An efficient method for aiming heliostats using ray-tracing,” in *Abstract, SolarPACES 2020*.